Annu. Rev. Fluid Mech. 1991. 23 : 81–106

HYDRAULICS OF ROTATING STRAIT AND SILL FLOW

L. J. Pratt

Department of Physical Oceanography, Woods Hole Oceanographic Institution, Woods Hole, Massachusetts 02543

P. A. Lundberg

Department of Oceanography, Göteborg University, Box 4038, S-400 40 Göteborg, Sweden

KEY WORDS: hydraulic control, straits, deep currents, hydraulic jumps

1. *Introduction*

The role of deep-water formation and spreading as an indicator and regulator of global climatic change has recently been emphasized in a number of investigations (e.g. Watts & Hayder 1983, Boyle & Keigwin 1987, Labeyrie et al 1987, Anderson & Lundberg 1988). Within this context, processes in the Atlantic Ocean have attracted the greatest attention, since both the Norwegian and the Weddell Seas (which constitute the world's two major areas where deep water is formed during wintertime convection) are located on the margins of this ocean basin (Wüst 1936).

The cold and dense water that fills the deeper parts of the Norwegian Sea escapes southward through two main passages: the Denmark Strait, and the Faroe Bank Channel. The deep-water outflow through the Denmark Strait (between Greenland and Iceland) over a comparatively shallow sill of depth ~ 600 m was known from the pioneering investigations at the turn of the century; it was, however, not studied in a systematic fashion until the 1960s (Mann 1969, Worthington 1969, Ross 1984). The existence of the Faroe Bank Channel, with a sill depth of 850 m, was unknown to Helland-Hansen & Nansen (1909), who stated that "no bottom water with low temperatures can anywhere get out of the Norwegian

0066–4189/91/0115–0081$02.00

Sea...." In contrast to the Denmark Strait, the Faroe Bank Channel not only serves as a conduit for intermediate-water masses but also permits an overflow of Norwegian Sea deep water proper. It was not discovered until British survey vessels undertook detailed echo soundings in the region during the early 1940s. Since then, much work has been carried out with the aim of quantifying the deep-water transport and clarifying the dynamics of the flow (cf Harvey 1961, Crease 1965, Dooley & Meincke 1981, Borenäs & Lundberg 1988, Saunders 1990). The fate of these deep- and intermediate-water masses once they have passed the Greenland-Scotland Ridge into the North Atlantic proper has also attracted considerable attention (cf Cooper 1955, Lee & Ellett 1965, Swift et al 1981, Swift 1984).

Conditions in the Southern Hemisphere differ somewhat from those described above, since the Weddell Sea deep water, which was first described by Brennecke (1921), is not topographically constrained immediately adjacent to its region of origin. The northward flow of Antarctic Bottom Water instead appears to be controlled by the Vema Channel (Hogg et al 1982), through which deep water of temperature less than 1°C makes its way to the bottom of the Brazilian Basin, and, in the vicinity of the equator, by the Ceara Abyssal Plain (Whitehead & Worthington 1982, Whitehead 1989a). Because of the great depths and relative inaccessibility of these passages, field work did not start here until quite recently.

The North Atlantic is also affected by a high-saline, deep-water inflow from the Mediterranean through the Strait of Gibraltar (cf Lacombe & Richez 1982), which has attracted long-standing attention from oceanographers, since it is so easily traceable. To round off this overview of the marginal seas of the Atlantic, it must also be mentioned that the deeper regions of the Caribbean are reached by an inflow of Atlantic water through the Jungfern-Anegada Passage (Stalcup et al 1975).

All of the Atlantic deep-water flows described above take place through passages or over sills of such lateral extent that rotation plays a major role in the dynamics, i.e. the flow is more or less in geostrophic balance. The transports, furthermore, are of crucial importance for determining the mass balances of the oceanic subbasins that they feed or drain. In each of the passages mentioned above, the deep current is an overflow; dense water spills over the sill in a manner analogous to flow over a weir or dam. This situation closely resembles the smaller scale phenomena that classically have been the objects of study within hydrology and engineering hydraulics, and hence it is somewhat surprising that the first attempt to extend the concepts of hydraulic flow into the realm of a rotating frame of reference was undertaken within a meteorological context (cf Houghton 1969). This anomalous situation was, however, soon rectified by Stern (1972), who pioneered the use of rotating hydraulics within oceanography,

and by Whitehead et al (1974), who not only looked at the dynamics of the flow per se but also discussed it in the wider context of basin mass balances and, finally, undertook a set of laboratory experiments. Since these early studies, the area of rotating hydraulics (defined as comprising field, laboratory, and theoretical research) has expanded rapidly. In the present review we broadly outline the subsequent developments and identify current gaps in our knowledge.

Due to limitations in space we restrict our discussion to flow in channels, thereby excluding related work on the hydraulics of coastal currents (Röed 1980, Hughes 1987, and references therein).

2. *Critical Flow, Upstream Influence, and Other Basic Concepts*

Although investigations of hydraulically driven flows are often restricted to steady currents, some discussion of time-dependent effects greatly aids one's intuition into the principles underlying critical control and upstream influence in these flows. One experiment that nicely illustrates these concepts involves a dam break. Consider a barrier mounted on an obstacle at position $y = 0$ and restraining fluid lying in the region $y < 0$, as shown in Figure 1*a*. If the barrier is suddenly removed the fluid over the obstacle

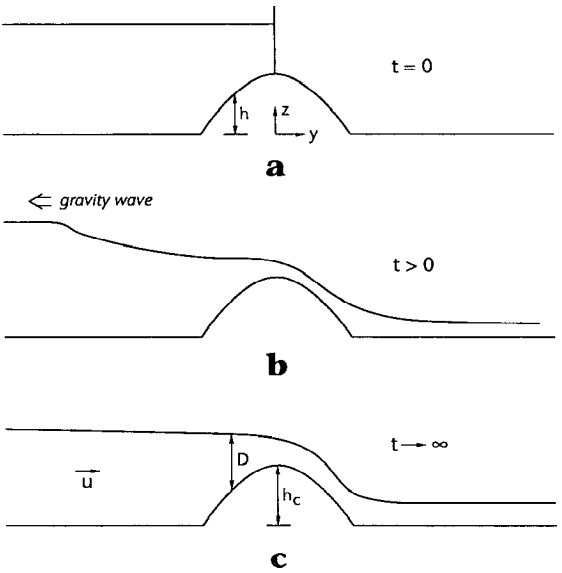

Figure 1 The flow produced by a dam break over an obstacle with (*a*) the initial conditions, (*b*) the transient state, and (*c*) the final steady flow.

will accelerate toward positive y and begin spilling over the sill. Gravity waves are generated that propagate toward negative y (Figure 1*b*), setting resting fluid in motion. Eventually, the free discharge reaches a steady state (Figure 1*c*).

Immediately after the barrier is broken the horizontal fluid velocity v at $y = 0$ (initially zero) begins to increase. What determines its final, steady value? The answer is suggested by consideration of the propagation speed of gravity waves at the sill. Initially these waves are able to propagate toward negative y, but they become retarded by the advection of the accelerating flow. Eventually, the advection becomes so strong that even the swiftest (the long gravity waves) cannot propagate upstream; the flow becomes critical. Denoting by v and D the horizontal velocity and depth, respectively, the critical condition occurs when $v = (gD)^{1/2}$, where g is the gravitational acceleration. Once critical flow is achieved, the conditions downstream of $y = 0$ are no longer sensed at the sill or at any point upstream. No further time evolution occurs at $y = 0$ because the downstream conditions (which originally were responsible for the time-dependent adjustment) are no longer felt.

Once a steady state has been established it is possible to relate the conditions at the sill to those upstream of the obstacle using the appropriate statements of mass and energy conservation. For a shallow, one-dimensional flow, the energy (or Bernoulli head) B_∞ and volume transport Q are conserved:

$$\frac{v^2}{2} + g(D+h) = B_\infty, \tag{1}$$

$$wvD = Q, \tag{2}$$

where h denotes the elevation of the bottom and w the channel width, both of which vary with y. Elimination of v between (1) and (2) leads to a single equation for the layer depth in terms of the constants B_∞ and Q and the geometric variable h:

$$\frac{Q^2}{2D^2w^2} + g(D+h) = B_\infty. \tag{3}$$

Equation (3) allows computation of the value of the depth for each $h(y)$ provided that the constants B_∞ and Q are known. A great deal of insight into the general behavior of the solutions is revealed by a plot of $B_\infty - gh$ as a function of D for a fixed flow rate Q (see Figure 2). As one moves in the y-direction the topographic height (and thus the value of $B_\infty - gh$) varies and the corresponding values of the scaled depth D can be read from the Figure 2 curve. It can be shown that the curve's minimum lies at

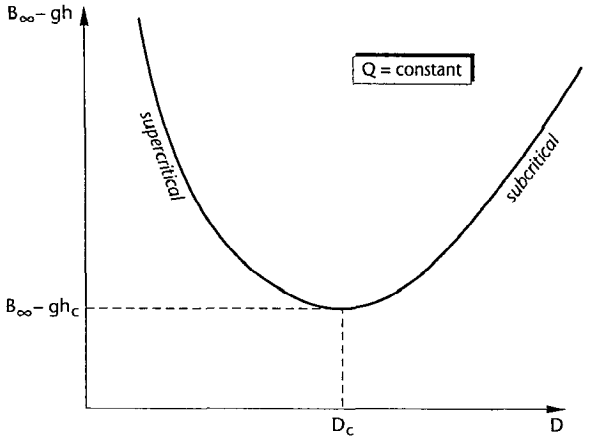

Figure 2 Plot of $B_\infty - gh$ vs D for constant Q [based on Equation (3)]. Note that $B_\infty - gh$ is a measure of the elevation of the bottom of the channel.

the critical value of D, so that critical flow can occur only at the sill. To the left of the minimum the flow is supercritical ($v^2 > gD$), and to the right the flow is subcritical ($v^2 < gD$).

Now suppose that the transport Q is known in advance. Then the depth D_c at the critical section is determined by

$$D_c = v_c^2/g = Q^2/w^2 D_c^2 g,$$

or

$$D_c = (Q^2/w^2 g)^{1/3}. \tag{4}$$

Substitution of D_c and Q into Equation (3) determines the constant B_∞ and allows a solution curve similar to that of Figure 2 to be constructed. For each value of h lying upstream and downstream of the sill, D can take on one of two values, corresponding to the subcritical and supercritical branches of the solution curve. For solutions having critical flow at the sill, it can be shown (Pratt 1984c) that the only stable configuration is with subcritical values upstream and supercritical values downstream of the sill. This choice gives a solution similar in appearance to that of Figure 1*c*, with fluid spilling over the sill.

Construction of the steady solution in the previous example required foreknowledge of the volume transport Q. It is also possible to construct the complete solution without previous knowledge of Q by solving an appropriate initial-value problem. This approach makes use of nonlinear long-wave theory to connect quiescent flow far upstream of the obstacle

to steady flow immediately upstream across the wave front excited by barrier removal (Figure 1*b*). This approach can be applied to a variety of initial-value problems, and Baines & Davies (1980) review the case in which the flow is set up by a towed obstacle. The transient field consists of regions of steady flow separated by hydraulic jumps, bores, and rarefaction waves. Using shock-joining and Riemann-invariant theory for shallow-water flow (Stoker 1957), it is possible to connect the steady regions and thereby piece together the entire transient solution.

In addition to the freely discharging solutions, there exist purely subcritical or supercritical flows. They can be established in the dam-break problem if fluid with a finite but slightly smaller depth initially exists to the right of the barrier. A steady state is reached as a result of the upstream and downstream water levels equilibrating, causing the pressure gradient at $y = 0$ to vanish. Such solutions are therefore symmetric in the sense that the free-surface elevation for any value of h upstream of the sill also occurs for the same h downstream of the sill. An example can be constructed using Figure 2 by varying h such that the minimum in the solution curve is not passed through. Long (1954, 1970) showed that purely subcritical or supercritical flows are achieved in towing experiments when the obstacle height is less than a threshold value determined by the towing speed and initial depth.

The fundamental difference between the free-discharge solutions and the purely subcritical or supercritical solutions lies in the role that the obstacle plays in regulating the flow. In the latter case, there is no regulation; the obstacle has no effect on the final steady state achieved other than determining the local shape of the free surface. In a towing experiment, for example, the final depth realized upstream of the moving obstacle is identical to the initial depth.

For a free-discharging flow, on the other hand, the upstream state is linked to the sill height. This link can be established by evaluating (1) at the sill and using the critical condition and statement of mass conservation (2). The resulting relation

$$\tfrac{3}{2}(gQ/w)^{2/3} = B_\infty - gh_c \tag{5}$$

shows that Q and B_∞ cannot be varied independently of the sill height h_c. We can think of Q and B_∞ as determined by the upstream conditions through

$$Q = v_u D_u w_u,$$

$$B_\infty = v_u^2/2 + gD_u,$$

where the subscript "u" denotes upstream. Thus, the upstream depth and

velocity cannot be varied independently of the sill height. If one attempts to vary v_u and D_u in a way that violates (5), then a transient response is triggered that acts to reestablish (5). This sequence of events involves a wave, generated upstream by the original change in v_u and h_u, which propagates downstream and is partially reflected from the obstacle. The reflected wave returns upstream and readjusts the values of v_u and D_u such that (5) is reestablished. (An example of this chain of events is given by Pratt 1984b.) The reflected wave is central to the phenomenon of upstream influence; it is the means by which the obstacle communicates with the upstream flow. We refer to flows having critical sections at which upstream influence is exercised as being critically or hydraulically controlled.

In addition to these features, there are a number of variational properties that distinguish critically controlled from noncontrolled flows. For example, it can be shown that the energy B of a controlled flow is a minimum for all possible flows having the same Q. Also, the volume transport Q is maximized over all solutions having the same B. Finally, for a given solution (given Q *and* B), critical flow occurs at the section where the *specific energy* $v^2/2+gD$ is minimized.

If the flow upstream of the sill originates from a deep reservoir or basin, so that $B_\infty \cong gD_u$, then Equation (5) becomes

$$Q = (\tfrac{2}{3}\Delta z)^{3/2} w g^{1/2}.$$

This "weir" formula gives the volume transport in terms of the elevation difference Δz between the upstream surface level and sill. It allows determination of Q through one relatively straightforward measurement.

The properties outlined above are features of a wide variety of critically controlled fluid flows in geophysics and engineering. Normally these "hydraulic-type" flows can be described by a single dependent variable d, which varies only with position along the conduit. One is free to choose d to be any convenient, physically significant quantity. The relationship between d and the geometric variables $h(y)$, $w(y)$, etc, describing the cross section of the conduit can be written

$$J[d; h, w, \ldots] = \text{constant}. \tag{6}$$

This relationship is multivalued in that d may take on several values for given w, h, etc. A merging of the different solution branches or roots occurs when

$$\partial J/\partial d = 0. \tag{7}$$

Gill (1977), who originally proposed this formalism, showed that (7) is fulfilled when the flow is critical with respect to one of the long-wave modes of the system. The physical interpretation is that a stationary

wave in the system indicates a continuum of steady-state solutions, each associated with a different amplitude. In the previous example, the Bernoulli equation (3) corresponds to (6), and the branch condition (7) occurs at the minimum of the Figure 2 solution curve, where the flow is critical.

The majority of theoretical treatments in rotating hydraulics are based on Gill's formalism; however, there *are* fluid flows that exhibit critical control but cannot be described by a relationship of the form (6) [see Pratt (1984a, 1986) for two examples].

3. *The Equations of Rotating Hydraulics*

The standard setting for investigations of rotating hydraulics is a rotating channel aligned in the y-direction and having bottom elevation $z = h(x, y)$ (Figure 3). In most cases, interest is confined to a single, homogeneous, moving layer of fluid with horizontal velocity components $u(x, y)$ and $v(x, y)$ in the x- and y-directions, respectively. The upper boundary $z = \eta$ of this layer can be treated as a free surface or an interface separating the stream from an inactive upper layer of slightly lower density. Since the majority of past treatments have assumed the channel cross section to be rectangular, we will take $\partial h/\partial x = 0$ unless otherwise indicated. The position of the side walls will be given by $x = \pm w/2$.

The fundamental assumption of hydraulics that allows formulation of the problem as in Equation (6) is that of gradual variations along the axis of the channel. The depth D is assumed to vary on a scale large compared with D itself, permitting the use of a shallow-water formalism. Also, the cross-sectional geometry is assumed to vary on a scale large compared with w. Assuming that the internal flow structures experience equally

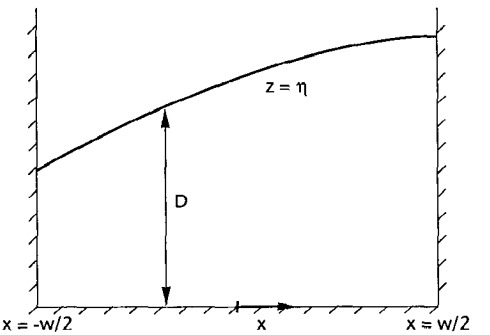

Figure 3 Definition sketch showing cross section of rotating channel.

gradual variations in the y-direction, then simple scale analysis shows the y-velocity to be geostrophically balanced:

$$fv = g'\eta_x, \tag{8}$$

where g' represents the gravitational acceleration reduced in proportion to the density difference across the interface, and f is the Coriolis parameter.

Additional constraints are provided by the statements of along-axis momentum balance and conservation of potential vorticity:

$$uv_x + vv_y + fu = -g\eta_y, \tag{9}$$

$$\frac{(f+v_x)}{D} = G(\psi), \tag{10}$$

where ψ is the transport stream function, defined by

$$\psi_y = -uD, \qquad \psi_x = vD. \tag{11a,b}$$

The assumption of gradual variations along the channel implies that $|u_y| \ll |v_x|$, and u_y has thus been neglected in the relative vorticity expression. The potential vorticity is sometimes written as

$$G(\psi) = f/D_0(\psi), \tag{12}$$

where D_0, the "potential" depth, is the thickness to which a water column must be stretched such that the relative vorticity vanishes.

It is sometimes convenient to use the Bernoulli equation

$$\frac{v^2}{2} + g'\eta = B(\psi), \tag{13}$$

where the assumption $|u| \ll |v|$ has been used to neglect the term $u^2/2$. It can be shown that the Bernoulli head and potential vorticity are related by $dB/d\psi = G$. Of the four relations (8), (9), (10), and (13), only three are independent.

4. *The Cross-Channel Structure*

The governing equations described above are "semigeostrophic" in that only the along-stream velocity v is geostrophically balanced. In practice the major simplification of semigeostrophy is that the cross- and along-channel structures of the flow field can be dealt with separately. To describe the former, Equations (8) and (10) can be combined, with the result

$$(g'/f^2)D_{xx} - D/D_0(\psi) = -1, \tag{14}$$

where we continue to regard h as constant, and where

$$\psi = \frac{g'}{2f}[D^2(y,x) - D^2(y,-w/2)], \tag{15}$$

as implied by (8) and (11b).

In deep overflows, $D_0(\psi)$ is influenced by deep-water formation processes. To date, only one extremely simple conceptual model has been suggested for determination of $D_0(\psi)$. Whitehead et al (1974) envision an upstream basin in which newly formed columns of deep water are set into horizontal motion sufficiently slow that the interface is nearly horizontal and the relative vorticity is much less than f. If the basin has a horizontal bottom, then $D = D_0 =$ constant. In the strait itself, the columns of bottom water are assumed to have been squashed by topographic effects to the point that $D/D_0 \ll 1$. The middle term in (14) then becomes insignificant, and the remaining equation can be solved, giving a parabolic depth profile. Since the first term in (14), which is $O(Dg'/f^2w^2)$, dominates the middle term, which is $O(D/D_0)$, it follows that $w^2 \ll (g'D_0)/f^2$ (i.e. w is much less than the Rossby radius of deformation based on D_0). The relative vorticity in the strait is $\cong f$ owing to the vortex-squashing effect. This model is mistakenly referred to as the zero-potential-vorticity limit, since the same solutions are obtained from (8) and (10) by setting $G(\psi) = 0$. In reality, it is dangerous to refer to the dimensional quantity $G(\psi)$ as small or zero; a more appropriate measure is the nondimensional ratio D/D_0. The parabolic depth profile is obtained for finite and even nonconstant $G(\psi)$ so long as $D/D_0(\psi) \ll 1$. We therefore suggest referring to the case with $D/D_0 \ll 1$ as the *deep-reservoir* limit and to the subcase of a horizontal upstream interface and $D/D_0 \ll 1$ as the WLK (Whitehead, Leetma & Knox 1974) model. In the latter the horizontal reservoir interface affords certain computational advantages.

It is also easy to solve (14) analytically for the case in which D_0 is a constant and D/D_0 is not small. As shown by Gill (1977), the solution describes a flow contained in sidewall layers of thickness $(g'D_0)^{1/2}/f$. The most realistic physical setting is one in which the reservoir is wide, but not deep, compared with the channel. The flow in the reservoir is confined to independent boundary layers, one on each sidewall, and the interior depth is D_0. In the channel the boundary layers overlap if the channel width w is less than about $2(g'D_0)^{1/2}/f$.

Figure 4 shows three types of cross-channel depth profiles predicted using the deep-reservoir limit [see Whitehead et al (1974) for details]. In the first case (Figure 4*a*) the depth is finite across the entire channel and the geostrophically balanced along-channel velocity v is positive (into the figure). In the second case (Figure 4*b*) the flow is separated from the left sidewall and extends a length L over the width. Simple scale analysis based on the geostrophic relation (Pratt 1987) suggests that

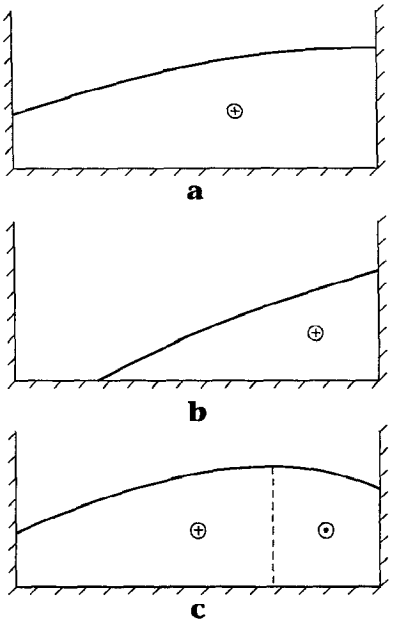

Figure 4 Cross sections showing different possible depth profiles for the case $D/D_0 \ll 1$. (*a*) Nonseparated, unidirectional; (*b*) separated, unidirectional; (*c*) nonseparated, with velocity reversal.

$$L = O\left\{\frac{2(g'\bar{D})^{1/2} f^{-1}}{\bar{U}/(g'\bar{D})^{1/2}}\right\}, \tag{16}$$

i.e. twice the ratio of the Rossby radius of deformation to a local Froude number (both quantities based on the average depth and velocity scales $\bar{U}$ and $\bar{D}$). If the local channel width w exceeds L, the flow is separated.

The final case (Figure 4*c*) is that of an attached flow having a velocity reversal ($v < 0$) along the right sidewall. An objection to this solution may be raised—namely, that specification of potential vorticity along streamlines of the reversed flow (which do not originate in the upstream basin) requires further assumptions. These (and possibly other) streamlines may originate from the "downstream" basin or may be part of a closed recirculation or eddy. The specification of potential vorticity in recirculations or regions of reversed flow remains an outstanding and relatively untouched problem, although Shen (1981) and Whitehead (1986) suggest treating such regions as stagnant. (This general problem of reversed flows is further exacerbated when account is taken of topographies that are more realistic than a rectangular channel.)

It is now apparent that the cross-channel structure of the flow is characterized by (at least) two intrinsic length scales. The first, $(g'D_0)^{1/2}/f$, is

the distance over which v decays from the sidewalls and might be called the "global" Rossby deformation radius. This length scale is determined by conditions in the upstream basin and is independent of y. The second, $(g'\bar{D})^{1/2}/f$, is associated with the width of the separated stream and might be called the "local" Rossby deformation radius.

The cross-channel structure equation (14) has not yet been solved for nonconstant D_0. Some of the technical difficulties impeding this calculation are discussed in Section 6.

5. *The Hydraulics (or Along-Channel Structure) of Flow With Uniform Potential Vorticity*

The along-channel structure of the flow is determined by the two y-dependent integration "constants" $C_1(y)$ and $C_2(y)$, which appear in the solution to the cross-channel structure equation (14). Two additional constraints are required to determine $C_1(y)$ and $C_2(y)$, and these can be selected from the following: First, the Bernoulli equation (13) can be applied at either sidewall or at the free boundary of a separated flow. Second, the y-momentum equation (9) can be applied at either sidewall or at the free boundary. Finally, the transport

$$Q = \int_{-w/2}^{w/2} vD\,dx$$

can be required to be constant. Only two of these possible five constraints are independent.

Once these steps have been taken, the mathematical problem for determining $C_1(y)$ and $C_2(y)$ becomes similar to that of determining v and D in one-dimensional, nonrotating hydraulics (Section 2). A polynomial for $C_1(y)$ or $C_2(y)$ [cf Equation (3)] can be found having parameters consisting of the geometrical variables $h(y)$ and $w(y)$ and three constants characterizing the upstream flow. In Gill (1977), the latter are chosen to be D_0, Q, and a third constant ψ_i measuring the partitioning of mass flux in the sidewall boundary layers of the reservoir. In the WLK model, D_0 is essentially infinite and ψ_i is replaced by h_u, the height of the reservoir interface over the sill. In each case, the polynomial gives a relationship of the form (6).

The solution to the polynomial can be plotted, resulting in curves similar to that of Figure 2. The curve contains two branches, one corresponding to supercritical and one to subcritical flow with respect to the long-wave modes of the system. When the flow remains attached (as in Figure 4*a*), the long waves are modified Kelvin waves having velocity and depth fields that decay from the lateral boundaries over a distance $(g'D_0)^{1/2}/f$. In the

WLK model one has $(g'D_0)^{1/2}/fw \gg 1$, and thus the wave fields extend across the full stream width. It is also possible for separation to occur from the left (facing downstream) wall, so that a free streamline forms at the left edge of the flow. Under this condition the left-wall Kelvin wave is replaced by a frontal wave (Stern 1980, Kubokawa & Hanawa 1984). In either case, the flow can become critical with respect to the appropriate wave. For uniform potential vorticity the critical condition is

$$\bar{U} = (g'\bar{D})^{1/2}[1 - T^2(1 - \bar{D}/D_0)]^{1/2},$$

where $\bar{U}$ and $\bar{D}$ denote the average of the values of u and D at the left and right edges of the stream, and

$$T = \tanh [wf/2(gD_0)^{1/2}]$$

(Gill 1977). When $wf/(g'D_0)^{1/2} \ll 1$, as in the WLK model, the critical condition reduces to $\bar{U} = (g'\bar{D})^{1/2}$, which is identical to the classical result $v = (g'D)^{1/2}$ when v and D are replaced by stream-edge averages.

When the flow remains attached to both sidewalls, hydraulically controlled solutions exist that exhibit most of the classical features discussed in Section 2. In particular, the flow is critical with respect to Kelvin waves at the sill (or narrowest section), and variational properties (including transport maximization) analogous to those of classical hydraulics exist. In more descriptive terms, the fluid spills over the sill, much as in nonrotating hydraulics. Strong transitions in cross-sectional properties, such as the distribution of mass flux, can also take place (Gill 1977), and the average cross-channel slope of the interface generally increases as the transition from subcritical to supercritical flow occurs. Some sample interface configurations are shown in Figures 8 and 9 of Gill (1977).

As in the nonrotating case it is possible to derive formulas relating the volume transport to Δz, the height of basin interface above the bottom elevation at the critical section, or to some other easily measurable quantity. In the WLK model the transport relation for attached flow is

$$Q = \left(\frac{2}{3}\right)^{3/2} wg'^{1/2} \left[\Delta z - \frac{f^2 w^2}{8g'}\right]^{3/2}. \tag{17a}$$

When $f \to 0$ the right-hand side reduces to the classical (nonrotating) expression. Note that the effect of rotation is to reduce the transport. Whitehead et al (1974) and Shen (1981) have found good agreement between the Q given by (17a) and laboratory values measured in experiments with attached flows. When the flow is separated at the critical section, the transport relation can be obtained by replacing w in Equation (17a) by the stream width L. In the WLK model one has $L = (2g'\Delta z/f^2)^{1/2}$,

a result that can also be obtained by setting $\bar{U}/(g'\bar{D})^{1/2} = 1$ and $\bar{D} = \Delta z/2$ in (16). Substitution into (17a) gives

$$Q = \frac{g'(\Delta z)^2}{2f}. \tag{17b}$$

In summary, the hydraulics of uniform-potential-vorticity flow closely parallels classical hydraulics as long as the stream remains attached to the sidewalls. When separation occurs, the situation becomes more complicated and interesting. To begin with, the dynamics of the frontal wave are drastically different from the dynamics of the Kelvin wave it replaces. (The frontal wave is characterized by large cross-channel velocities, whereas the corresponding velocity in a Kelvin wave is zero.) Furthermore, Pratt & Armi (1987) have shown that when the flow is critical with respect to this new wave, a stagnation point occurs at the right sidewall, a result that is independent of the potential-vorticity distribution. They further speculate that a reversed circulation must exist in the subcritical flow upstream, as shown in Figure 5. This situation does occur in the deep-upstream-basin limit, with depth profiles upstream of the critical section resembling that of Figure 4*c*. Here the flow is subcritical and reversed at the right wall.

This situation was investigated experimentally by Shen (1981), who set up a critically controlled rotating flow in a laboratory channel. For sufficiently large rotation rates, separation was induced downstream of the control section (a combination of sill and width contraction). As rotation was further increased, the separation point moved upstream (nearer the critical section), and, at a sufficiently high rotation rate, the separation point reached a critical section and ceased moving upstream. At this point

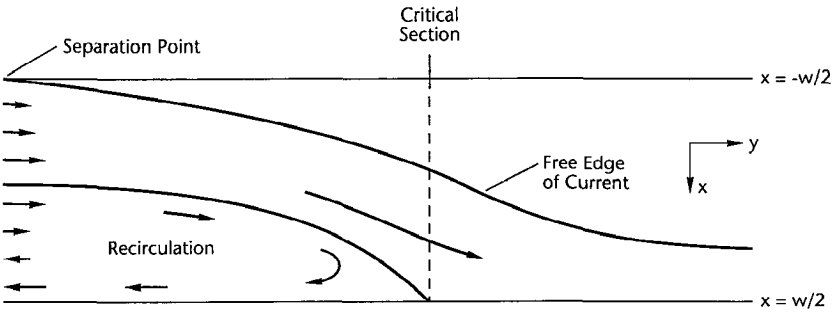

Figure 5 Plan view showing separated flow at the critical section with a corresponding stagnation point on the opposite wall. A recirculation exists upstream.

agreement between the predicted and the observed transport began to break down, and there was some indication of a recirculation upstream of the control section. These findings suggest that the flow resists being critically controlled by frontal-wave dynamics. Furthermore, the appearance of a recirculation suggests that the potential vorticity may no longer have been entirely specified by the "deep-basin" limit. Closed streamlines may have allowed the value of D_0 to become significantly modified by bottom friction. As yet, no model has been presented that satisfactorily treats recirculations, and no model has been put forth showing why the flow upstream of the sill cannot separate. Finally, it is worth underlining that the general problem of flow reversals becomes even more pronounced when a more realistic topography than that provided by a rectangular channel is taken into account. Any natural cross-sectional geometry will be characterized by the depth D vanishing at the horizontal delimitation points of the flow. From Equations (10) and (12) it is recognized that under these constraints, the flow in the region of the right bank is particularly apt to experience negative velocities in order to conserve potential vorticity (Borenäs & Lundberg 1986, 1988).

Several attempts at relaxing the assumption of gradual along-channel variations have been made. Sambuco & Whitehead (1976) considered the case of an infinitely wide sill, taking $\partial D/\partial x = 0$. Their model is interesting but probably not relevant to wide channels, where the flow is banked against one of the sidewalls and separated from the other. Pratt (1984a) considered the higher order corrections to Gill's model that occur for slow but finite variations in cross-section geometry. When the basic flow is close to criticality, these variations lead to wavelike steady flows governed by a nonlinear dispersive equation. Solutions are restricted, however, to cases where the amplitudes of variation in w and h are small. It remains unknown how well the basic features of rotating hydraulic theory are preserved when rapid variations in cross section occur.

It must be noted that in many practical oceanographic applications, interest is not primarily focused on understanding the dynamic subtleties of the flow, but rather is directed toward obtaining quantitative estimates of deep-water fluxes through passages under what generally are presumed to be controlled conditions. The WLK model has frequently been applied for this purpose and in many cases appears to do "zeroth-order justice" to the transports. Whitehead (1989b) has compared the observed Q to that predicted by (17) for the overflows of the Denmark Strait, Iceland-Faroe Ridge, Vema Channel, and Ceara Abyssal Plain, finding that the theory overestimates the observations by 160–400%. The discrepancies can be attributed to numerous idealizations (inviscid flow, layered stratification, etc) made in the theory, but the crude agreement is promising.

Borenäs & Lundberg (1986) have examined the effects of using a more realistic topography than the rectangular one generally favored in hydraulic studies. A direct comparison between critically controlled flows of equal cross-sectional area through a rectangular and a parabolic channel, respectively, showed that for geophysically reasonable choices of the governing parameters, the rectangular-channel-controlled transport only exceeds that through a parabolic constriction by 50–100%. [This comparison was undertaken for a situation with a finite depth of the upstream basin, i.e. a case differing from that treated by Whitehead et al (1974), but this discrepancy is of minor importance within the context of examining the direct effects of the local channel topography.]

Use of the patently erroneous assumption of an infinitely deep upstream basin evidently does not induce any grave errors into the hydraulic analysis. Arguments favoring this state of affairs have recently been put forth by Whitehead (1989b), who based his analysis on a heuristic extension of the classical deep-upstream-basin, rectangular-channel WLK model. (Results of a similar nature can, more formally, be obtained by parameter expansions of the full nonzero, constant-potential-vorticity problem for a rectangular or parabolic channel.)

The deep-upstream-basin model must hence be regarded as a useful tool in many situations of practical oceanographical interest. As a caveat, however, it must be underlined that when specific details of the flow such as its cross-channel structure are examined, the simplified model may reveal certain shortcomings. This was recently pointed out by Rydberg (1980) in his analysis of the Bornholm Strait and Faroe Bank Channel overflows and by Saunders (1990) in his study of the deep-water flow from the Norwegian Sea through the Faroe Bank Channel. These objections may, on the other hand, in practice be completely overshadowed in the analysis by the formal problems that upper-layer motion and nonstationarity of the deep-water flow produce (Borenäs & Lundberg 1990).

6. *Nonuniform Potential Vorticity*

When $D_0(\psi)$ is nonconstant, the cross-channel structure equation (14) is nonlinear and, aside from the special case $D/D_0 \ll 1$, no solutions (analytic *or* numerical) have appeared in the literature. Nevertheless, any solution to the second-order equation must contain two integration "constants" containing the y-dependence. The mathematical problem for the along-channel structure of the flow may therefore be cast in traditional form. Pratt & Armi (1987) used this fact to extend a number of traditional hydraulic features to the nonuniform $D_0(\psi)$ case. For example, it was shown that critical flow can occur only at a point of vanishing bottom slope ($\partial h/\partial y = 0$) in a channel of constant width and (with one exception)

at a point of extreme width ($\partial w/\partial y = 0$) in a channel with a horizontal bottom. They further suggested ways of formulating the problem in terms of Gill's functional $J[D; h, w, \ldots]$ and showed that $\partial J/\partial D = 0$ is a condition for critical flow.

Stern (1974) also discussed a generalized critical condition based on a minimization principle equivalent to $\partial J/\partial D = 0$. His criterion for critical flow in a stream with general potential vorticity was

$$\int_{-w/2}^{w/2} (v^2 D)^{-1}[1 - v^2/g'D]\, dx = 0. \tag{18}$$

This condition implies that the local Froude number $v^2/g'D$ must be unity for some value in the range $-w/2 < x < w/2$.

The primary dynamical complication resulting from nonuniformity of $D_0(\psi)$ is the presence of additional wave modes associated with the potential-vorticity-gradient restoring mechanism. These "potential-vorticity" waves (related to Rossby waves) give rise to additional modes of criticality and critical control. To investigate the consequences of multiple wave modes, Pratt & Armi (1987) considered a *nonrotating* flow ($\partial D/\partial x = 0$) in which the potential vorticity (now equal to v_x/D) is given by $G_0 - a\psi$, with a and G_0 constant. In this case, the cross-channel structure of the velocity v is determined by

$$v_{xx} + aD^2(y)v = 0. \tag{19}$$

For $a < 0$ the potential vorticity gradient is directed to the right, facing downstream, and potential-vorticity waves (which tend to propagate with high potential vorticity to their right) move in the same direction as the volume transport. The only wave that can become stationary in the flow is the gravity mode, and there is only one critically controlled steady state. The solution curve for this case resembles that of Figure 2 (with a single lobe).

For $a > 0$ the direction of the potential-vorticity gradient is reversed, allowing propagation of potential-vorticity waves against the flow. Multiple critically controlled states are now possible for any positive transport, and a unique specification of the steady flow no longer exists. The solution curve now has multiple lobes (Figure 6), each corresponding to a critically controlled solution with respect to a unique wave mode. Lobe #1 pertains to the case of gravity-wave control, whereas the other lobes correspond to potential-vorticity-wave control. Pratt & Armi (1987) suggest that the solution controlled by the gravity mode may be preferred on the basis of stability. Resolution of the nonuniqueness problem will, however, require a laboratory experiment or solution to an appropriate initial-value problem.

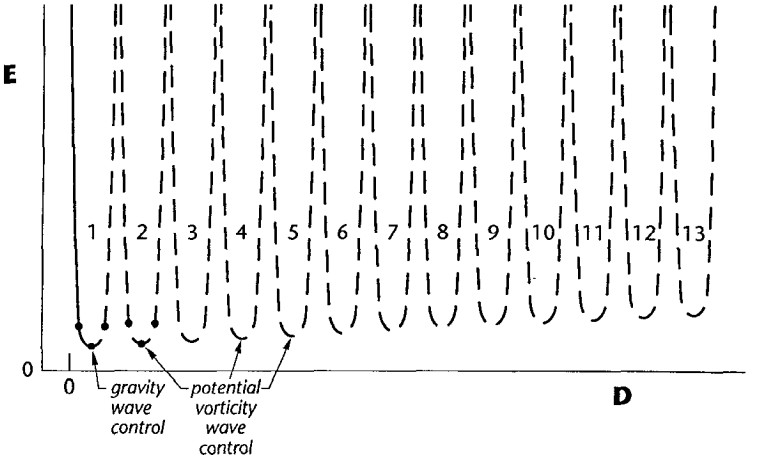

Figure 6 Solution curves for the nonrotating, nonuniform potential-vorticity flow considered by Pratt & Armi (1987). D is the fluid depth, E is a measure of the elevation of the bottom of the channel, and the volume transport is held fixed. (The interpretation of the curve is the same as in Figure 2.) Dashed lines represent solutions having velocity reversals.

From an observational point of view, the most striking feature distinguishing potential-vorticity-wave control from gravity-wave control is the presence in the former of velocity reversals at the control section. In Figure 6 solutions with velocity reversals are indicated by dashed lines. It can be seen that reversals occur at the minima of all curves save that of lobe #1. Velocity reversals at the control section have not been observed in the majority of observations of deep overflows, suggesting the gravity (or Kelvin) wave as the preferred mode of control. One exception is the Vema Channel overflow (Hogg et al 1982).

As yet, no solutions to the full cross-stream structure equation (14) have been found for nonconstant $D_0(\psi)$. It is possible to reduce (14) to a first-order equation by applying the integrating factor D_x, leading to

$$(D_x)^2 + 2f^2 D/g' = B(\psi), \tag{20}$$

so that

$$\int_{D(-w/2)}^{D(x)} [B(\psi) - 2f^2 D/g']^{-1/2}\, dD = x + w/2. \tag{21}$$

The problem now becomes one of specifying $B(\psi)$ [rather than $D_0(\psi)$] such that the integration in (21) can be performed analytically. The choice $B \propto \psi$ yields the constant-potential-vorticity model, since $dB/d\psi = G$. The

choice $B \propto \psi^2$, on the other hand, allows expression of the solution in terms of elliptic integrals, which must be regarded as a promising result.

7. *Rotating Jumps, Bores, and Time Dependence*

Internal jumps and bores (shocks) arise naturally in a number of straits, including the Windward Passage (Sturges 1975), the Strait of Gibraltar (La Violette & Arnone 1988), and Knight Inlet (Farmer & Smith 1980). Ranging from strongly turbulent discontinuities in the interfacial or isopycnal depth to smooth, undular transitions, jumps and bores can cause significant mixing and energy dissipation. Shocks are also important in the computation of time-dependent strait and sill flows, such as in the dam-break and towing problems described earlier. In these calculations segments of steady flow separated by (stationary) jumps or (moving) bores are pieced together using shock-joining theory. The solutions are extremely useful in developing one's intuition about upstream influence and conditions under which control can be established. Unfortunately, this approach has not yet been extended to rotating flows owing to the lack of a satisfactory shock-joining theory.

To describe the difficulty, we first review the principles behind shock joining in nonrotating channels. In one-dimensional shallow flows the joining is based on conservation of the transport and the total momentum flux, or "flow force." For a shock moving at speed c these constraints result in the Rankine-Hugoniot conditions

$$c[vD] - \left[v^2 D + \frac{g}{2} D^2 \right] = 0, \tag{22}$$

$$c[D] - [vD] = 0, \tag{23}$$

where the brackets denote jumps in the indicated quantities. For a hydraulic jump ($c = 0$), Equations (22) and (23) specify the depth and velocity on the downstream side given the depth and velocity on the upstream side.

In rotating-channel flows, bores and jumps have a two-dimensional structure that greatly complicates the shock-joining problem. Early investigations of rotating shocks (Yih et al 1964, Houghton 1969, Williams & Hori 1970) utilized geometries that rendered the flow one dimensional. However, the influence of sidewalls in rotating channels leads to two-dimensional effects in practically all cases of interest. As an example, consider the rotating hydraulic jump produced in the numerical solutions of Pratt (1983). As shown in Figure 7, the depth discontinuity is largest on the left (facing downstream) wall of the channel and decays over a distance on the order of the global deformation radius.

A logical starting point for a rotating-shock theory would be con-

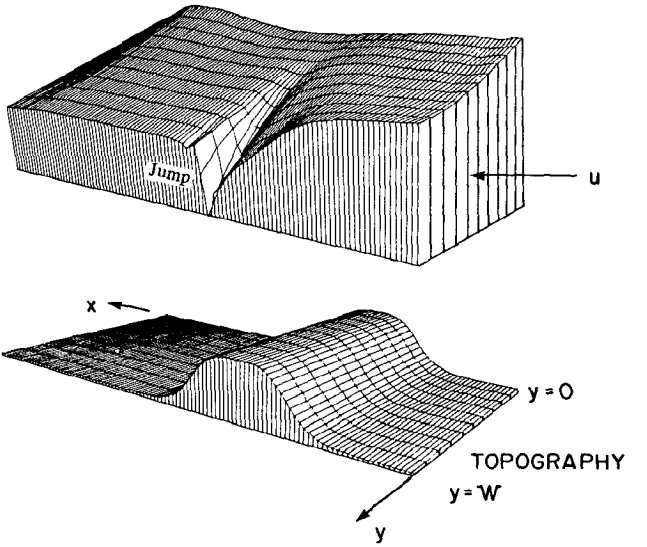

Figure 7 Hydraulic jump produced in a numerical model (Pratt 1983). The flow is from right to left, and the upper frame shows the free-surface (or interface) deformation produced when the channel flow passes over the obstacle shown in the lower frame.

servation laws for the cross-sectionally integrated transport and flow force. If the potential vorticity of the flow is known in advance, these two laws could be used to constrain the two integration constants in the solution to the cross-channel structure equation. The situation would then be comparable with the nonrotating case; for example, given the flow on the upstream side of a hydraulic jump, one could determine the downstream depth and velocity profile.

The problem with this approach is that potential vorticity can change across a shock. Pratt (1983) has shown that this change is given locally by

$$[G] = (1/VD)\,\frac{\partial}{\partial s}\,\{[D]^3/D_A D_B\},$$

where A and B denote points lying immediately on either side of the shock, and VD is the mass flux normal to the shock at any point. The change in potential vorticity thus depends on the tangential structure of the discontinuity. One requires foreknowledge of this structure to compute $[G]$ and close the shock-joining problem. Thus, the downstream potential vorticity is not necessarily known even if it is known upstream.

Nof (1984) and Pratt (1987) have formulated shock-joining theories based on the assumption that the $[G]$ is zero everywhere. However, Nof

(1986) has cast doubt on this approach by finding a special class of shocks in which the depth discontinuity occurs along a line perpendicular to the channel axis. This simplification allows one to compute the upstream and downstream end states *and* the potential vorticity jump. It is found that the jump in G can be as large as the upstream value of G itself.

In summary, the general shock-joining problem for a bore or jump in a rotating channel remains unsolved. Given an upstream flow and a shock speed, there is no available means of computing the downstream flow without *ad hoc* assumptions or a detailed analysis of the shock interior.

Until recently, all investigations of rotating jumps involved flows of finite depth. As discussed earlier, it is possible for the fluid to separate from the left sidewall (facing downstream) of a rectangular channel. One might ask whether a shock can exist in such a flow, particularly in view of the fact that shocks in attached flows have similarities with Kelvin waves. (As previously discussed, separation from the left wall removes one of the Kelvin waves.)

To investigate shock existence in a rotating, separated flow, Pratt (1987) set up a hydraulic jump in a laboratory channel and rotated the channel swiftly enough to cause separation of the supercritical flow immediately upstream of the jump. Although the upstream flow separated, the downstream (subcritical) flow did not, so that the fluid reattached at the original position of the jump. As the rotation rate was increased further, the supercritical flow narrowed, occupying a decreasing fraction of the channel width, whereas the subcritical flow remained attached. At the same time the depth jump decreased at all points along the depth discontinuity, so that the shock evolved into a lateral hydraulic jump, i.e. the main discontinuity became one in stream *width* rather than *depth*.

Despite the fact that rotating shocks were found in the laboratory experiments of Whitehead et al (1974), Sambuco & Whitehead (1976), Shen (1981), Whitehead (1986), and Pratt (1987), little is known about their interior structure. Experiments with better flow visualization and more complete velocity and depth measurements are needed.

8. *Density Stratification*

There are a number of oceanographically important overflows having vertical structures too complicated to be treated by single- (or $1\frac{1}{2}$-) layer hydraulic models.We do not have space to discuss the considerable body of literature that exists on multilayer or continuously stratified nonrotating flows. [The reader is referred to Armi & Farmer (1986) and Baines & Davies (1980) for recent advances and a review of this subject.] A number of rotationally influenced deep overflows exhibit structures too com-

plicated to be explained using $1\frac{1}{2}$-layer stratification. One example occurs in the Vema Channel (Hogg et al 1982, 1983), where the flow appears to have a $2\frac{1}{2}$- or three-layer character. Investigations dealing with the effects of rotation are at an initial stage, and most calculations have been limited to two-layer flows.

Dalziel (1988) has formulated the equations describing two-layer flow in a channel of rectangular cross section, each layer having uniform potential vorticity. The overall physical picture is rich, complicated, and obscured by formidable algebra. Complete solutions have been discussed for only a few simple cases, the most notable being a rotating exchange problem. Whitehead et al (1974) treat the case in which the "deep-reservoir" limit is in effect for both layers and the layer transports are equal and opposite. Dalziel (1990) has extended the geometry of this case to include a sill and identified the critically controlled solution having maximal exchange. As long as the interface between the two layers remains attached to the sidewalls, the solutions remain directly analogous to those of the classic nonrotating lock-exchange problem (as to be expected from our discussion of attached $1\frac{1}{2}$-layer flow). Further, it is possible to identify maximal and submaximal, critically controlled solutions as well as "virtual" and "sill" controls, all features of the nonrotating counterpart. Rotation causes a decrease in the exchange transport and can lead to separation of the interface from the sidewalls at the sill. The latter situation occurs when the channel width becomes less than the local internal Rossby radius. At larger rotation rates the exchange transport is independent of the channel width. Rotation also causes a stronger coupling to occur between layers, so that the effects of a sill on the lower layer are more easily transmitted to the upper layer. Whitehead et al (1974) have experimentally verified the exchange-transport prediction pertaining to a nonsill geometry for both separated and nonseparated cases.

Pratt & Armi (1990) have attempted to consider the effect of unequal transports (i.e. a net barotropic flow). The global internal Rossby radius of deformation is assumed much smaller than the channel width, and the baroclinic part of the flow is consequently confined to thin boundary layers. The barotropic flow is forced directly by width contractions and, in turn, forces the baroclinic boundary current in two independent ways. The dual nature of the baroclinic forcing gives rise to structures that are more complex than the channel geometry alone might indicate and leads to a new type of critical control.

An important complication introduced in multilayer models is that one density interface can "intersect" another, a phenomenon observed by Hogg et al (1982) in the Vema Channel and reproduced in a three-layer

hydraulic model (Hogg 1983). Hogg argues that this internal separation almost always accompanies hydraulic control. Flow reversals also can occur in his solutions (and in the models cited), but it is not clear how they are related to internal separation.

9. *Future Problems*

In the course of this discussion we have mentioned several research problems that beg consideration in the immediate future. These include the development of a satisfactory shock-joining theory for rotating jumps and bores, a method of computing the potential vorticity in recirculations, and a clearer assessment of the dynamical complications associated with density stratification and nonuniform potential vorticity. In addition, there are a number of pressing issues that bear on the hydraulics of rotating *and* nonrotating flows. The first issue concerns the relevance of concepts like critical control in time-dependent flows. Applications include the Strait of Gibraltar exchange flow, which is strongly modulated by tides, and the Denmark Strait overflow, which is known to be time varying (Mann 1969, Worthington 1969). The second concerns a more complete consideration of upstream conditions in overflow models. Upstream influence by a sill presumably affects deep-water formation processes, which in turn influence the potential vorticity, energy, and transport of the overflow. The interplay between the sill dynamics and the deep-water formation processes is an issue that has not yet been considered in analytic or laboratory models, save the overmixing model of Bryden & Stommel (1984).

A third major gap in our knowledge concerns the role of bottom and interfacial friction in critical control processes. Simple scale arguments indicate that bottom friction is significant in the Denmark Strait and Iceland-Scotland overflows (Pratt 1986). In rotating flow, bottom friction can lead to qualitative changes in the hydraulics of the flow, including shifts in the position of the control section; however, direct analogies still appear to exist with the frictionless case. In addition, bottom friction alters the potential vorticity of the flow in complicated ways, possibly leading to essential changes in the nature of the control problem.

To end this review on the same applied note as it was commenced, it may be worthwhile to summarize the urgent observational tasks in the Atlantic Ocean that confront the oceanographic community as regards the study of deep-water flows of mainly polar origin. There can hardly be any doubt that a study of the northward Antarctic Deep Water flow must be assigned a high priority in this context, motivated both by its climatological implications and by the interesting dynamic phenomena that have been

observed (Hogg 1983, Whitehead 1989a). The relative inaccessibility and great depths have hitherto precluded more extensive field programs in the pertinent "choke-point" areas, but presumably this situation will be rectified in the not too distant future. The prospects for a more precise quantification and an associated enhanced understanding of the dynamics of the other major deep-water inflows to the Atlantic proper are, on the other hand, much brighter. The high-saline deep-water flux from the Mediterranean through the Strait of Gibraltar has already been studied during a large-scale international field program in the 1980s (Almazan et al 1989). The exchanges with the Norwegian Sea have previously been investigated fairly extensively and will, furthermore, be subjected to a long-term monitoring effort in the course of the forthcoming World Ocean Circulation Experiment WOCE (Anonymous 1988). Nordic researchers have assumed the overall investigative responsibility for a section to roughly coincide with the Greenland-Scotland Ridge, comprising (among other things) the deep-water flows through the Faroe Bank Channel and the Denmark Strait.

As the spatial resolution that may be achieved during oceanographic field work has become increasingly fine meshed, it has also been recognized that many of the passages connecting minor deep-ocean basins with the major Atlantic basins also offer interesting examples of well-defined deep-water flows (cf the Charlie Gibbs Fracture Zone, the Discovery Gap, and the Romanche Fracture). As a consolation to those researchers whose interests primarily are focused toward dynamical studies rather than on climatologically relevant large-scale fluxes of cold bottom waters, it must be pointed out that a large number of conveniently located smaller scale passages provide fine opportunities for dedicated field studies aimed at clarifying various aspects of the mechanics of rotating deep-water flows. Geographically widely dispersed examples of such straits that recently have been investigated are the Bornholm Gap (Petrén & Walin 1976), the mouth of the Chesapeake Bay (Whitehead 1989b), Funka Bay, Hokkaido (Miyake et al 1988), and the mouth of Spencer Bay (Bye & Whitehead 1975).

ACKNOWLEDGMENTS

Many of the ideas presented herein were developed through discussions with Karin Borenäs, and we wish to acknowledge her input. Partial financial support was provided by the Woods Hole Oceanographic Institution through an independent study award and by the Swedish Natural Research Council under contract G-GU-4768. We also wish to thank Lisa Wolfe for preparing the manuscript.

Literature Cited

Almazan, J. L., Bryden, H., Kinder, T., Parilla, G., eds. 1989. *Seminario sobre la Oceanografia del Estrecho de Gibraltar*. Madrid: Soc. Esp. Estud. Comun. Estrecho Gibraltar. 567 pp.

Andersson, L. S., Lundberg, P. A. 1988. Delayed albedo effects in a zero-dimensional climate model. *J. Atmos. Sci.* 45: 2294–2305

Anonymous. 1988. World Ocean Circulation Experiment implementation plan. *WMO/TD No. 242*, World Meteorol. Organ., Wormley, Engl.

Armi, L., Farmer, D. M. 1986. Maximal two-layer exchange through a contraction with barotropic net flow. *J. Fluid Mech.* 164: 27–51

Baines, P. G., Davies, P. A. 1980. Laboratory studies of topographic effects in rotating and/or stratified fluids. In *Orographic Effects in Planetary Flows. GARP Publ. Ser. No. 23*, pp. 233–99. Geneva: World Meteorol. Organ.

Borenäs, K. M., Lundberg, P. A. 1986. Rotating hydraulics of flow in a parabolic channel. *J. Fluid. Mech.* 167: 309–26

Borenäs, K. M., Lundberg, P. A. 1988. On the deep-water flow through the Faroe Bank Channel. *J. Geophys. Res.* 93(C2): 1281–92

Borenäs, K. M., Lundberg, P. A. 1990. Some questions arising from the application of hydraulic theory to the Faroe Bank Channel deep-water flow. *Pure Appl. Geophys.* In press

Boyle, E. A., Keigwin, L. 1987. North Atlantic thermohaline circulation during the past 20,000 years linked to high-latitude surface temperature. *Nature* 330: 35–40

Brennecke, W. 1921. Die Ozeanographischen Arbeiten der Deutschen Antarktischen Expedition. 1911–12. *Arch. Dtsch. Seewarte* 39: 1–216

Bryden, H. L., Stommel, H. M. 1984. Limiting processes that determine basic features of the circulation in the Mediterranean Sea. *Oceanol. Acta* 7(3): 289–96

Bye, J. A. T., Whitehead, J. A. 1975. A theoretical model of the flow in the mouth of Spencer Gulf, South Australia. *Estuar. Coast. Mar. Sci.* 3: 477–81

Cooper, L. H. N. 1955. Deep water movements in the North Atlantic as a link between climatic changes around Iceland and biological productivity of the English Channel and the Celtic Sea. *J. Mar. Res.* 14: 347–62

Crease, J. 1965. The flow of Norwegian Sea water through the Faroe Channel. *Deep-Sea Res.* 12: 143–50

Dalziel, S. B. 1988. *Two-layer hydraulics: maximal exchange flows*, PhD thesis. Univ. Cambridge, Engl.

Dalziel, S. B. 1990. Rotating two-layer sill flows. In *The Physical Oceanography of Sea Straits. NATO-ASI Ser.*, ed. L. J. Pratt. Dordrecht: Kluwer. In press

Dooley, H., Meincke, J. 1981. Circulation and water masses in the Faroese Channels during Overflow-73. *Dtsch. Hydrogr. Z.* 34: 41–55

Farmer, D. M., Smith, J. D. 1980. Tidal interaction of stratified flow with a sill in Knight Inlet. *Deep-Sea Res.* 27A: 239–54

Gill, A. E. 1977. The hydraulics of rotating-channel flow. *J. Fluid Mech.* 80: 641–71

Harvey, J. G. 1961. Overflow of cold deep water across the Iceland-Greenland Ridge. *Nature* 189: 911–13

Helland-Hansen, B., Nansen, F. 1909. The Norwegian Sea. *Fiskeridir. Skr. Ser. Havunders.* 2(1): 1–390

Hogg, N. G. 1983. Hydraulic control and flow separation in a multi-layered fluid with application to the Vema Channel. *J. Phys. Oceanogr.* 13: 695–708

Hogg, N. G., Biscaye, P., Gardner, W., Schmitz, W. J. 1982. On the transport and modification of Antarctic Bottom Water in the Vema Channel. *J. Mar. Res.* 40: 231–63

Houghton, D. D. 1969. Effect of rotation on the formation of hydraulic jumps. *J. Geophys. Res.* 74: 1351–60

Hughes, R. L. 1987. The role of higher shelf modes in coastal hydraulics. *J. Mar. Res.* 45: 33–58

Kubokawa, A., Hanawa, L. 1984. A theory of semigeostrophic gravity waves and its application to the intrusion of a density current along a coast. Part I. Semigeostrophic gravity waves. *J. Oceanogr. Soc. Jpn.* 40: 247–59

Labeyrie, L. D., Duplessy, J. C., Blanc, P. L. 1987. Variations in mode of formation and temperature of oceanic deep waters over the past 125,000 years. *Nature* 327: 477–82

Lacombe, H., Richez, C. 1982. The regime of the Strait of Gibraltar. In *Hydrodynamics of Semi-Enclosed Sea* ed. J. C. J. Nihoul, pp. 13–73. Amsterdam: Elsevier

La Violette, P. F., Arnone, R. A. 1988. A tide-generated internal waveform in the western approaches to the Strait of Gibraltar. *J. Geophys. Res.* 93: 15,653–67

Lee, A., Ellett, D. 1965. On the contribution of overflow water from the Norwegian Sea to the hydrographic structure of the North Atlantic Ocean. *Deep-Sea Res.* 12: 129–42

Long, R. R. 1954. Some aspects of the flow of stratified fluids. II. Experiments with a two-fluid system. *Tellus* 6: 97–115

Long, R. R. 1970. Blocking effects in flow over obstacles. *Tellus* 22: 471–80
Mann, C. R. 1969. Temperature and salinity characteristics of the Denmark Strait overflow. *Deep-Sea Res.* 16: 125–37
Miyake, H., Tanaka, I., Murakami, T. 1988. Outflow of water from Funka Bay, Hokkaido, during early spring. *J. Oceanogr. Soc. Jpn.* 44: 163–70
Nof, D. 1984. Shock waves in currents and outflows. *J. Phys. Oceanogr.* 14: 1683–1702
Nof, D. 1986. Geostrophic shock waves. *J. Phys. Oceanogr.* 16: 886–901
Petrén, O., Walin, G. 1976. Some observations of the deep flow in the Bornholm Strait during the period June 1973–December 1974. *Tellus* 28: 74–87
Pratt, L. J. 1983. On inertial flow over topography. Part 1. Semigeostrophic adjustment to an obstacle. *J. Fluid Mech.* 131: 195–218
Pratt, L. J. 1984a. On inertial flow over topography. Part 2. Rotating channel flow near the critical speed. *J. Fluid Mech.* 145: 95–110
Pratt, L. J. 1984b. A time-dependent aspect of hydraulic control in straits. *J. Phys. Oceanogr.* 14: 1414–18
Pratt, L. J. 1984c. On nonlinear flow with multiple obstructions. *J. Atmos. Sci.* 41: 1214–25
Pratt, L. J. 1986. Hydraulic control of sill flow with bottom friction. *J. Phys. Oceanogr.* 16: 1970–80
Pratt, L. J. 1987. Rotating shocks in a separated laboratory channel flow. *J. Phys. Oceanogr.* 17: 483–91
Pratt, L. J., Armi, L. 1987. Hydraulic control of flows with nonuniform potential vorticity. *J. Phys. Oceanogr.* 17: 2016–29
Pratt, L. J., Armi, L. 1990. Two-layer rotating hydraulics: strangulation, remote and virtual controls. *Pure Appl. Geophys.* In press
Rŏed, L. P. 1980. Curvature effects on hydraulically driven inertial boundary currents. *J. Fluid Mech.* 96: 395–412
Ross, C. K. 1984. Temperature-salinity characteristics of the "overflow" water in the Denmark Strait during "OVERFLOW '73." *Rapp. P.-V. Réun. Cons. Int. Explor. Mer* 185: 111–19
Rydberg, L. 1980. Rotating hydraulics in deep-water channel flow. *Tellus* 32: 77–89
Sambuco, E., Whitehead, J. A. 1976. Hydraulic control by a wide weir in a rotating fluid. *J. Fluid Mech.* 73: 521–28
Saunders, P. M. 1990. Cold outflow from the Faroe Bank Channel. *J. Phys. Oceanogr.* 20: 29–43
Shen, C. Y. 1981. The rotating hydraulics of open-channel flow between two basins. *J. Fluid Mech.* 112: 161–88
Stalcup, M. C., Metcalf, W. G., Johnson, R. G. 1975. Deep Caribbean inflow through the Anegada-Jungfern Passage. *J. Mar. Res.* 33: 15–35
Stern, M. E. 1972. Hydraulically critical rotating flow. *Phys. Fluids* 15: 2062–64
Stern, M. E. 1974. Comment on rotating hydraulics. *Geophys. Fluid Dyn.* 6: 127–30
Stern, M. E. 1980. Geostrophic fronts, bores, breaking and blocking waves. *J. Fluid Mech.* 99: 687–703
Stoker, J. J. 1957. *Water Waves.* New York: Interscience. 567 pp.
Sturges, W. 1975. Mixing of renewal water flowing into the Caribbean Sea. *J. Mar. Res.* 33: 117–30 (Suppl.)
Swift, J. H. 1984. The circulation of the Denmark Strait and Iceland-Scotland overflow waters in the North Atlantic. *Deep-Sea Res.* 28: 1107–29
Swift, J. H., Aagaard, K., Malmberg, S.-A. 1981. The contribution of the Denmark Strait overflow to the deep North Atlantic. *Deep-Sea Res.* 27: 29–42
Watts, R. G., Hayder, M. E. 1983. Climatic fluctuations due to deep-ocean circulation. *Science* 219: 387–88
Whitehead, J. A. 1986. Flow of a homogeneous rotating fluid through straits. *Geophys. Astrophys. Fluid Dyn.* 36: 187–205
Whitehead, J. A. 1989a. Surges of Antarctic Bottom Water into the North Atlantic. *J. Phys. Oceanogr.* 19: 853–61
Whitehead, J. A. 1989b. Internal hydraulic control in rotating fluids—applications to oceans. *Geophys. Astrophys. Fluid Dyn.* 48: 169–92
Whitehead, J. A., Leetma, A., Knox, R. A. 1974. Rotating hydraulics of strait and sill flows. *Geophys. Fluid Dyn.* 6: 101–25
Whitehead, J. A., Worthington, L. V. 1982. The flux and mixing rates of Antarctic Bottom Water within the North Atlantic. *J. Geophys. Res.* 87(C10): 7903–24
Williams, R. T., Hori, A. M. 1970. Formation of hydraulic jumps in a rotating system. *J. Geophys. Res.* 75: 2813–21
Worthington, L. V. 1969. An attempt to measure the volume transport of Norwegian Sea overflow water through the Denmark Strait. *Deep-Sea Res.* 16: 421–32
Wüst, G. 1936. Schichtung und Zirkulation des Atlantischen Ozeans; das Bodenwasser und die Stratosphäre. In *Wissenschaftlische Ergebnisse der Deutschen Atlantischen Expedition auf dem Forschungs- und Vermessungsschiff "Meteor" 1925–1927*, ed. A. Defant, VI:1. Berlin: de Gruyter & Co.
Yih, C. S., Gascoigne, H. E., Debler, W. R. 1964. Hydraulic jump in a rotating fluid. *Phys. Fluids* 7: 638–42

Annual Review of Fluid Mechanics
Volume 23, 1991

CONTENTS

(*continued*)